

# HYDROGEN ABSORBABILITY IMPROVEMENT OF TI-BASED QUASICRYSTAL WITH MAGNESIUM POWDER SYNTHESIZED BY MECHANICAL ALLOYING PROCESS

Jittima Varagul<sup>1</sup>, Nitirut Phongsirimethi<sup>2</sup>, Somsak Siwadamrongpong<sup>1,\*</sup>, Akito Takasaki<sup>3</sup>, Susumu Uematsu<sup>3</sup>, and Alicja klimkowicz<sup>4</sup>

*Received: April 01, 2020; Revised: August 18, 2020; Accepted: August 21, 2020*

## Abstract

Hydrogen is an interesting choice as alternative energy due to promising properties: clean, environmentally friendly, as well as being one of the most exuberant elements on earth. Nowadays, various materials and methods have been proposed as hydrogen storage by many researchers. Ti-based quasicrystal alloy (Ti-Zr-Ni) was reported as excellent hydrogen storage materials with 140 sites of interstices, which are higher than the number of sites found in other crystals. As well as magnesium (Mg), is known as one of the most famous hydrogen reservoir materials due to the lower cost and good stability when reacting with hydrogen. However, the enthalpy and temperature hydrogen absorption were quite high of MgH<sub>2</sub> and reports on Ti-Zr-Ni-Mg alloys were limited. In order to improve the capacity of hydrogen storage, this research has been conducted by adding Mg into the Ti-Zr-Ni quasicrystal alloy as Ti<sub>43</sub>Zr<sub>38</sub>Ni<sub>17</sub>Mg<sub>2</sub>. The samples were mixed by mechanical alloying under two conditions (1) 600 rpm with 20 h milling time and (2) 630 rpm with 30 h milling time. The samples were annealed to form quasicrystal. The gas-phase hydrogen absorption has been observed by pressure composition isotherm (PCT) measurements. Morphology and structural analysis were analyzed by XRD and SEM. The measurements showed the maximum capacity achieved by 600 rpm with 20 h milling time. The hydrogen-to-metal (H/M) of the former

---

<sup>1</sup> School of Manufacturing Engineering, Institute of Engineering, Suranaree University of Technology, Nakhon Ratchasima, Thailand. E-mail: jittima@sut.ac.th, somsaksi@sut.ac.th

<sup>2</sup> School of Mechanical and Process System Engineering, Institute of Engineering, Suranaree University of Technology, Nakhon Ratchasima, Thailand. E-mail: tony.nitirut@gmail.com

<sup>3</sup> Department of Engineering Science and Mechanics, Institute of Engineering, Shibaura institute of Technology, Toyosu, Japan. E-mail: takasaki@shibaura-it.ac.jp, uematsu@shibaura-it.ac.jp

<sup>4</sup> SIT Research Laboratory, Institute of Engineering, Shibaura institute of Technology, Toyosu, Japan. E-mail: alicja.klimkowicz@gmail.com

\* Corresponding author

condition has revealed a higher capacity of hydrogen storage with H/M = 1.99 than the latter condition with H/M = 1.58.

**Keywords:** Quasicrystal, mechanical alloying, hydrogen storage, magnesium

## Introduction

The quasicrystal has a new type of translational long-range order and rotational symmetry. The quasicrystal contain more tetrahedral interstitial sites than normal crystals due to the structure has Bergman two-shell atomic cluster. The reports indicated that Bergman two-shell cluster contains 20 tetrahedral interstitials within its inner shell and 120 between its inner and outer shells (Morozov *et al.*, 2006; Takasaki and Kelton, 2006). A large number of interstices were also found in the icosahedral quasicrystal (i-phase) and these interstices may become appropriate sites for hydrogen storage. This result was consistent with the result reported by Tominaga *et al.* (2015) which icosahedral quasicrystal was appropriate properties for hydrogen storage.

Quasicrystal was discovered by Shechtman *et al.* (1984). It has been found in an aluminum alloy and later has been found to be thermodynamically stable in many alloys (Shechtman *et al.*, 1984; Takasaki and Kelton, 2006; Samavat *et al.*, 2012). One of the most famous compounds was Ti-based quasicrystal (Ti-Zr-Ni). Ti-based quasicrystal was the second largest group of the stable quasicrystals, which was the thermodynamic stable, strong in chemical affinity with hydrogen and inexpensive. Especially, Ti<sub>45</sub>Zr<sub>38</sub>Ni<sub>17</sub> showed a very high hydrogen storage capacity. Which hydrogen concentration hydrogen-to-metal ratio (H/M) was 1.30 (Tominaga *et al.*, 2015). There were mainly two phases in Ti-based quasicrystal; (i) icosahedral quasicrystal and (ii) crystal phase (Ti<sub>2</sub>Ni). Icosahedral quasicrystal could contain a large number of tetrahedral interstices which could absorb more hydrogen than normal crystals as mentioned earlier. For crystal phase (Ti<sub>2</sub>Ni), it could contain several of interstitial sites for hydrogen storage (Xiangyu *et al.*, 2010). However, the crystal phase (Ti<sub>2</sub>Ni) was sensitive to react with oxygen,

thus controlling the oxygen in the process became a critical parameter (Takasaki and Kelton, 2006).

Magnesium (Mg) was known as one of the most famous hydrogen reservoir materials, in the form of MgH<sub>2</sub>, due to its low cost and good stability when reacting with hydrogen. The magnesium hydride (MgH<sub>2</sub>) has high thermodynamic stability to storage hydrogen of 7.6 wt% (Jain *et al.*, 2010; Wang and Wang, 2017). However, the enthalpy and temperature for hydrogen absorption were very high. In 2017, Wang has reported that there were many methods for improving magnesium hydride including (i) alloying (ii) nano scaling (iii) nanoconfinement (iv) adding catalysts and (v) mixing with other metal hydrides (Wang and Wang, 2017).

When Magnesium was added into a Ti-based quasicrystal structure, Mg<sub>2</sub>Ni crystal phase was reported to appear after the annealing process (Reilly and Wiswall, 1968; Zaluski *et al.*, 1995). The crystallized phase (Mg<sub>2</sub>Ni) was one of the most important hydrogen storage materials. The advantage of Mg<sub>2</sub>Ni was high hydrogen capacity up to 3.6 wt% (Zaluski *et al.*, 1995). It was also reported that hydrogen-absorbing of Mg<sub>2</sub>Ni has relatively high kinetic compare to other forms of Mg crystals. However, Mg<sub>2</sub>Ni cannot absorb hydrogen under normal conditions. The usual hydrogenation condition of Mg<sub>2</sub>Ni was between 250°C and 350°C for hydrogen-absorbing.

The authors have also carried out the investigation of quasicrystal phase appearing in Ti-based Ti-Zr-Ni-Mg compound (Niturut *et al.*, 2019). There was reported that the icosahedral and crystal phases were formed from Ti<sub>43</sub>Zr<sub>38</sub>Ni<sub>17</sub>Mg<sub>2</sub> compound which revealed high potential as hydrogen storage material. Therefore, in this research, pressure composition isotherm (PCT) measurements

were performed to obtain the hydrogen-to-metal ratio (H/M) of  $\text{Ti}_{43}\text{Zr}_{38}\text{Ni}_{17}\text{Mg}_2$  compound produced by the mechanical alloying process.

## Materials and Methods

Commercially pure powders Ti (99.9%), Zr (99.9%), Ni (99.9%), and Mg (99.9%) were used as starting materials for mixing of the sample with the chemical composition of  $\text{Ti}_{43}\text{Zr}_{38}\text{Ni}_{17}\text{Mg}_2$ . A mixture compound was mechanically alloyed by the mechanical alloying (MA) process in a planetary ball mill machine (Fritsch Pulverisette-7). The commercially pure powders were poured into the stainless-steel vials with five stainless steel milling balls (15 mm in diameter). The MA process was carried out under argon atmosphere to avoid the oxidation of the samples because the oxidation could reduce the potential of hydrogen storage. The total mass of the powder mixture for MA was 10.383 g which consisted of Ti 3.253 g, Zr 5.478 g, Ni 1.576 g and Mg 0.076 g. The mass of mixed powder was calculated from a ball-to-powder ratio of 8:1, which suitable for intermediate ball-milling conditions: medium milling energy (Zaluska *et al.*, 1999; Takasaki and Kelton, 2006). The MA process was conducted for two conditions; (1) the rotation speed of 600 rpm with 20 h (Tominaga *et al.*, 2015) and (2) the rotation speed of 630 rpm with 30 h (Azuha *et al.*, 2020) shown in Table 1.

After the MA process, the samples have been supposed to be amorphous phases. Thus, the samples were then annealed at annealing temperature, shown in Table 1, for a period of 2 h (Takasaki *et al.*, 2002; Takasaki and Kelton, 2006), in a high vacuum of  $\geq 1.00 \times 10^{-4}$  Pa by a turbo molecular pump (Azuha *et al.*, 2020). The phase transformation from amorphous to form icosahedral quasicrystal phase (i-phase) was expected. The annealing temperature was

achieved from Differential scanning calorimetry (DSC) measurements. DSC measurements were carried out between room temperature and desired temperature using a scan rate of  $5^\circ\text{C}\cdot\text{min}^{-1}$  under an argon atmosphere. The annealing temperature was conducted at  $500^\circ\text{C}$  for the sample from the rotation speed of 600 rpm with 20 h and  $550^\circ\text{C}$  for the rotation speed of 630 rpm with 30 h.

The XRD pattern of the sample after the MA process, after annealing and after hydrogen absorption could be identified by X-ray diffraction (XRD) measurement using Rigaku SmartLab with  $\text{Cu-K}\alpha$  radiation at 30 kV and 40 mA. The surface morphology of the samples before and after PCT were observed by Scanning Electron Microscope (SEM), model JEOL/JSM-7610F (Azuha *et al.*, 2020).

The hydrogen absorption and desorption pressure-composition isotherms (PCT) were measured at a constant temperature of 573 K (Takasaki and Kelton, 2006) by a Sieverts-type apparatus. The vessel that has a hydrogen-free sample inside was heated by an electric heater and kept constant at 573 K. After that, the hydrogen gas was gradually released by the PCT program control. In case that the sample could absorb hydrogen during pressure increase, the pressure will be dropped, and additional hydrogen will be loaded until the pressure become stable. The hydrogen absorption capacity (H/M ratio) will be determined from the total pressure change (Kim *et al.*, 1999; Tominaga *et al.*, 2015).

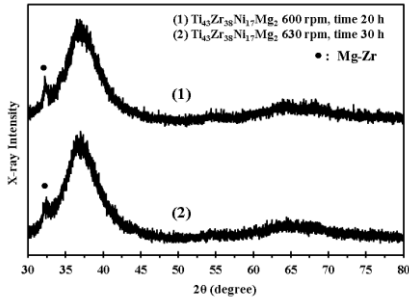
## Results and Discussion

Figure 1 shown the X-ray diffraction (XRD) patterns of mechanically alloyed  $\text{Ti}_{43}\text{Zr}_{38}\text{Ni}_{17}\text{Mg}_2$ . Both conditions could be observed in almost all amorphous phase. Please note that in the range  $2\theta$  of 30-35 deg. a tiny peak of Magnesium-Zirconium Alloy (Mg-Zr) phase

**Table 1. Materials composition and the annealing temperature obtained from DSC analysis**

Composition	Conditions	Parameters		Annealing Temperature ( $^\circ\text{C}$ )
		Speed (rpm)	Milling time (h)	
$\text{Ti}_{43}\text{Zr}_{38}\text{Ni}_{17}\text{Mg}_2$	(1)	600	20	550
	(2)	630	30	500

was observed. The results were in accordance with the previous works that the i-phase could not be obtained outright after the MA process (Takasaki and Kelton, 2006). Determination of the annealing temperature could be obtained from the onset temperature of the DSC peak



**Figure 1.** XRD patterns for  $\text{Ti}_{43}\text{Zr}_{38}\text{Ni}_{17}\text{Mg}_2$  powders after mechanical alloying process

- (1)  $\text{Ti}_{43}\text{Zr}_{38}\text{Ni}_{17}\text{Mg}_2$  Rotation speed 600 rpm, time 20 h,  
 (2)  $\text{Ti}_{43}\text{Zr}_{38}\text{Ni}_{17}\text{Mg}_2$  Rotation speed 630 rpm, time 30 h

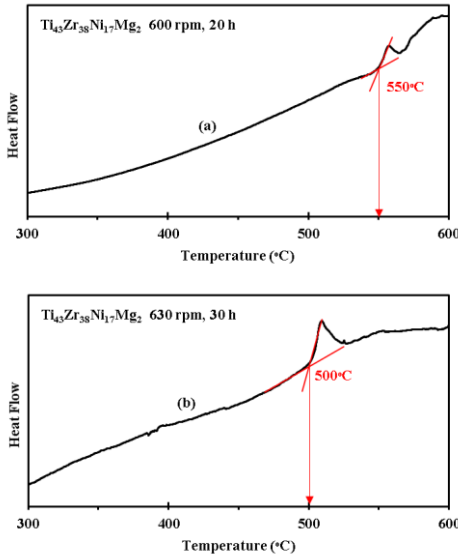


**Figure 2.** Differential scanning calorimetry for  $\text{Ti}_{43}\text{Zr}_{38}\text{Ni}_{17}\text{Mg}_2$  powders after mechanical alloying

- (2a)  $\text{Ti}_{43}\text{Zr}_{38}\text{Ni}_{17}\text{Mg}_2$  at 600 rpm 20 h,  
 (2b)  $\text{Ti}_{43}\text{Zr}_{38}\text{Ni}_{17}\text{Mg}_2$  at 630 rpm 30 h,

results because the onset-temperature should suffer unchanged when peak-temperature shifts due to heating rate and sample mass. (Fucke *et al.*, 2010; Floriano *et al.*, 2013). From the DSC curve, condition 1 showed the onset temperature of the crystallization at 550°C (Figure 2(a)) and the temperature of 500°C (Figure 2(b)) was observed for condition 2. Table 1 summarized the observed temperature at each condition for the annealing process.

From Table 1, it was clearly demonstrated that the annealing temperature of conditions 2 was lower than that of condition 1. Higher rotational speed and a longer time for milling of powders might yield smaller particle sizes of the compounds so that the transformation temperature of the amorphous phase becomes lower. Figure 3 shows the morphology of particle, the condition 1 (average particle of size 46.77  $\mu\text{m}$ ) was generally larger than that of the condition 2 (average particle of size 38.75  $\mu\text{m}$ ). It was also reported that the small

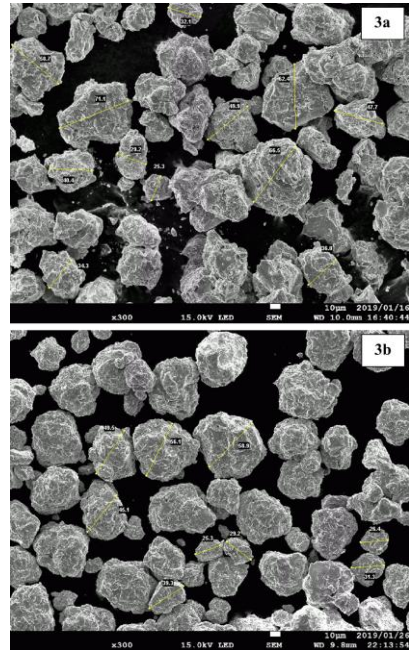


**Figure 3.** Particles of size by SEM measurements (3A)  $\text{Ti}_{43}\text{Zr}_{38}\text{Ni}_{17}\text{Mg}_2$  compound with 600 rpm with 20 h milling time, (3B)  $\text{Ti}_{43}\text{Zr}_{38}\text{Ni}_{17}\text{Mg}_2$  compound with 630 rpm with 30 h milling time

particle size might lead to lower hydrogen absorption capacity than large particles size (Chung and Perng, 2003; Rongeat and Roué, 2004). It was discussed due to the small particles might stable with oxide than large particles and yield in the reduction of hydrogenation rate (Zaluska *et al.*, 1999).

Figure 4 displayed the XRD patterns of  $Ti_{43}Zr_{38}Ni_{17}Mg_2$  after the annealing process. It has appeared that the i-phase was observed in both conditions (Takasaki and Kelton, 2006). Two types of crystal phases including  $Ti_2Ni$  and  $Mg_2Ni$  were observed. The i-phase in the  $Ti_{43}Zr_{38}Ni_{17}Mg_2$  compound could be observed in both conditions in the two thetas of 35-40 degrees and 65 degrees. However, the peaks at about 44 degrees and 76-78 degrees were implied that rotation speed of 600 rpm with

20 h milling time was yielded a higher amount of i-phases than a rotation speed of 630 rpm with 30 hours milling time. Therefore, from the viewpoint of the i-phase amount, the  $Ti_{43}Zr_{38}Ni_{17}Mg_2$  compound with 600 rpm with 20 h milling time results in a slightly higher amount than  $Ti_{43}Zr_{38}Ni_{17}Mg_2$  compound with 630 rpm with 30 hours milling time. On the other hand, crystal phases ( $Ti_2Ni$  and  $Mg_2Ni$ ) were observed for both conditions. Thus, based on the results, that could be implied that  $Ti_{43}Zr_{38}Ni_{17}Mg_2$  compound with 600 rpm with 20 h milling time showed better potential as hydrogen storage materials by considering from amount of i-phase appearing. After the annealing process, samples were brought into the hydrogenation process by PCT. The result of the hydrogen to metal ratio (H/M) at 573 K showed that the maximum H/M ratio was about 1.99 for  $Ti_{43}Zr_{38}Ni_{17}Mg_2$  compound with 600 rpm with 20 h milling time (condition 1). It was obviously higher than the H/M ratio of 1.58 for  $Ti_{43}Zr_{38}Ni_{17}Mg_2$  compound with 630 rpm with 30 h milling time (condition 2) as shown in Figure 5. This results provided evidence that conditions 1 of MA could absorb hydrogen more than that of MA condition 2. The hydrogen to metal (H/M) ratio could be obtained by the following equation; proposed by Viano *et al.* (2010).

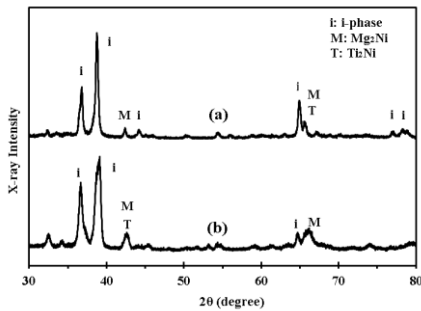


**Figure 4. XRD patterns for  $Ti_{43}Zr_{38}Ni_{17}Mg_2$  powders after annealing**  
**(4a)  $Ti_{43}Zr_{38}Ni_{17}Mg_2$  Rotation speed 600 rpm, time 20 h, Temp 550°C,**  
**(4b)  $Ti_{43}Zr_{38}Ni_{17}Mg_2$  Rotation speed 630 rpm, time 30 h, Temp 500°C**

$$\frac{H}{M} = \frac{a_q^H - a_q^0}{0.1974} \quad (1)$$

From the equation,  $a_q^H$  represents quasi-lattice parameter at the hydrogen concentration of interest and  $a_q^0$  measured quasi-lattice parameter for the non-hydrogenated i-phase. The value 0.197 was measured from a slope of the quasi-lattice that expands linearly with hydrogen concentration. The X-ray patterns of the sample after hydrogenation was shown in Figure 6. From Deriving Bragg's Law to explain the interference pattern of X-rays scattered by crystals could be obtained by the following equation.

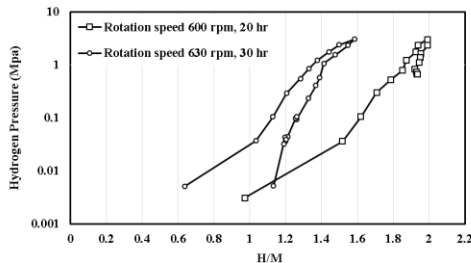


**Figure 5. Hydrogen absorption and desorption pressure-composition**

$$n\lambda = 2d\sin\theta \quad (2)$$

where  $n$  is a parameter of integer,  $\lambda$  is the wavelength of the X-rays,  $d$  is the spacing between planes in the atomic lattice of the sample and  $\theta$  is the diffraction angle in degrees (Elton and Jackson, 1966). So considers

between a high peaks positions of i-phase (110000i) in Figure 6(b) (before hydrogenation) and Figure. 6(c) (after hydrogenation). It could be seen that the shift of i-phase peak after hydrogenation. If comparing the lattice

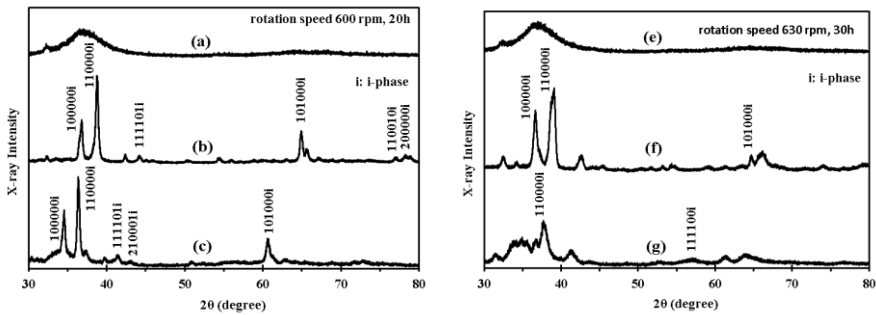


**Figure 6.** X-ray diffraction patterns for the i-phase powder Rotation speed 600 rpm, 20h: (6a) before annealing process, (6b) after annealing process, (6c) after pressure-composition isotherm (PCT) measurements at 573 K and rotation speed 630 rpm, 30h: (6e) before annealing process, (6f) after annealing process, (6g) after pressure-composition isotherm (PCT) measurements at 573 K

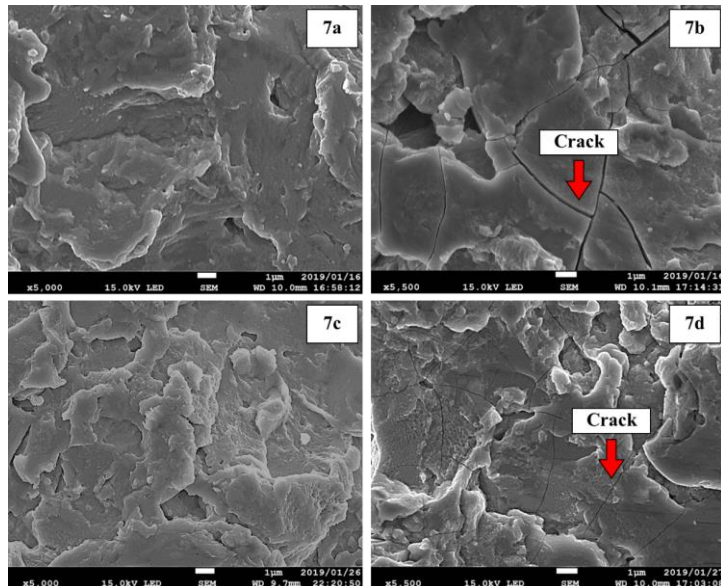


**Figure 7.** Result of SEM analysis to compare the surface morphology of compounds before and after hydrogenation process.

(7a) before hydrogenation of  $\text{Ti}_{43}\text{Zr}_{38}\text{Ni}_{17}\text{Mg}_2$  Rotation speed 600 rpm, 20 h  
 (7b) after hydrogenation of  $\text{Ti}_{43}\text{Zr}_{38}\text{Ni}_{17}\text{Mg}_2$  Rotation speed 600 rpm, 20 h  
 (7c) before hydrogenation of  $\text{Ti}_{43}\text{Zr}_{38}\text{Ni}_{17}\text{Mg}_2$  Rotation speed 630 rpm, 30 h  
 (7d) after hydrogenation of  $\text{Ti}_{43}\text{Zr}_{38}\text{Ni}_{17}\text{Mg}_2$  Rotation speed 630 rpm, 30 h

parameter of spacing between planes in the atomic lattice of the sample, it could be found the expansion of the lattice after hydrogenation approximately 5.87 % for the MA condition of 600 rpm and 20 hours. It was found to larger than the expansion of the lattice for MA condition of 630 rpm with 30 h which the expansion of the lattice was approximately 3.00%. The expansion of the lattice after hydrogenation could be considered due to the insertion of hydrogen into the lattice, which agrees with the evidence as described by SEM results in Figure 7. The similar results were also found in previous work (Takasaki and Kelton, 2006). Figure 7 exhibited the morphology before and after hydrogenation of the samples. It was found that crack has appeared after hydrogenation, it may be induced by lattice volume expansion (Diego *et al.*, 2008; Balcerzak, and Jurczyk, 2015). Figure 7(b) (condition 1) could be considered the larger and deeper crack comparing with the cracks on the sample of condition 2 as indicated in Figure 7(d). This evidence was in accordance with to higher expansion according to alongside the higher value of H/M ratio. Other works have reported that TiNi alloy ( $Ti_2Ni$ ) has hydrogen storage ability up to 0.83 H/M, Nobuki *et al.* (2019), and Ti-Ni-Mg alloy could rise H/M ratio up to 1.6, Mori *et al.* (2007). It was implied that Mg might play an important role to enhance hydrogen absorbability. Therefore, it might be discussed that the higher hydrogen storage capacity in this work could be discussed because of magnesium doping into the Ti-based alloy with the appropriated mechanical alloying condition as shown in Table 2.

Desorption of hydrogen from the sample of condition 1 seem not to release hydrogen as low as pressure compared with the sample of

condition 2, as shown in Figure 5. It might be discussed as the phase change of the i-phase after hydrogen absorption and cause to irreversible lattice expansion which exhibited in a shift of the peak after the 1<sup>st</sup> hydrogenation as shown in Figure 6 and cracks in Figure 7. To confirm the hysteresis of hydrogen absorption and desorption of Ti-Zr-Ni-Mg alloy, the 2<sup>nd</sup> hydrogenation test should be carried out in further study.

## Conclusions

This research was undertaken to investigate the formation of icosahedral quasicrystal (i-phase) and crystal phases of mixed materials between Ti-based quasicrystals (Ti-Zr-Ni) and Magnesium (Mg) by using a mechanical alloying (MA) process, and capacity of hydrogen storage, hydrogen-to-metal (H/M) was also investigated. MA process was conducted under two conditions; (i) rotation speed of 600 rpm with 20 h milling time and (ii) rotation speed of 630 rpm with 30 h milling time. The following conclusion can be drawn from this study:

(1) The  $Ti_{43}Zr_{38}Ni_{17}Mg_2$  compound after MA was transformed from amorphous to icosahedral and crystal phases after the annealing process.

(2) The  $Ti_{43}Zr_{38}Ni_{17}Mg_2$  compound with 600 rpm with 20 h milling time was yielded high capacity for hydrogen storage with hydrogen-to-metal ratio (H/M) of 1.99 which was higher than that compound with 630 rpm with 30 h milling time.

(3) The higher capacity of hydrogen storage might be influenced by Mg doping into Ti-Zr-Ni system with an appropriated mechanical alloying condition.

**Table 2. Estimated the hydrogen to metal atom (H/M) ratio with that of the other Ti-based i-phases**

Composition	Parameters		H/M	Authors
	Speed (rpm)	Milling time (h)		
$Ti_{45}Zr_{38}Ni_{17}$	600	20	1.30	Tominaga and Takasaki <i>et al.</i> (2015)
$Ti_{43}Zr_{38}Ni_{17}Mg_2$	600	20	1.99	This work
$Ti_{43}Zr_{38}Ni_{17}Mg_2$	630	30	1.58	This work

## Acknowledgments

This work was supported by Amal Azraai Azuha and Keisuke Onoda. We greatly appreciate their generous help. The financial support and facilities that were provided by the Suranaree University of Technology and Shibaura Institute of Technology were also deeply appreciated.

## References

- Azuha, A.A., Klimkowicz, A., and Takasaki, A. (2020). Quaternary Quasicrystal Alloys for Hydrogen Storage Technology. *MRS Advances.*, 5(20):1,071-1,083.
- Balcerzak, M. and Jurczyk M. (2015). Influence of Gaseous Activation on Hydrogen Sorption Properties of TiNi and Ti<sub>2</sub>Ni Alloys. *J. of Materials Eng. Perform.*, 24(4):1,710-1,717.
- Chung, S.-R. and Perng, T.-P. (2003). Effect of particle size on hydrogenation properties of a gas-atomized AB<sub>5</sub>-type alloy. *J. Alloys Comp.*, 353(1-2):289-294.
- Diego, E., Srinivasan, S., Goswami, Y. and Stefanakos, E. (2008). Hydrogen storage behavior of ZrNi<sub>70/30</sub> and ZrNi<sub>30/70</sub> composites. *J. Alloy Comp.*, 458:223-30.
- Elton, L. and Jackson, D.F. (1966). X-ray diffraction and the Bragg law. *American J. Phys.*, 34(11):1,036-1,038.
- Fucke, K., Steed J., and Anderson k. (2010). Differential scanning calorimetry (DSC). Engineering & Physical Sciences Research Council (EPSRC) and Durham University, United Kingdom: Fucke K. <http://www.hydrateweb.org>. 2010.
- Floriano, R., Leiva, D.R., Deledda, S., Hauback, B.C., and Botta, W.J. (2013). Nanostructured MgH<sub>2</sub> obtained by cold rolling combined with short-time high-energy ball milling. *Mat. Res.*, 16(1):158-163.
- Jain, I.P., Chhagan, L., and Ankur J. (2010). Hydrogen storage in Mg: A most promising material. *Int. J. Hydro. Energy*, 35:5,133-5,144.
- Kim, J.Y., Gibbons P.C., and Kelton K.F. (1999). Hydrogenation of Pd-coated samples of the Ti-Zr-based icosahedral phase and related crystalline phases. *J. Alloys Comp.*, 5:589-592.
- Mori, R., Kikuchi, S., Tanaka, K., Takeichi, N., Tanaka, H., Kuriyama, N., Ueda, T.T., and Tsukahara, M. (2007). Hydrogenation characteristics of Mg based alloy prepared by super lamination technique. *Mat. Sci.*, p. 1,609-1,612.
- Morozov, A., Yu., Isaev, É I., and Vekilov, Y.K. (2006). Charge state and diffusion of hydrogen in the TiZrNi icosahedral alloy. *J. Phys. Solid State.*, 48:1,625-1,628.
- Nitirut, P., Somsak, S., Jittima, V., Takasaki, A., Uematsu, S., and Alicja, K. (2019). Appearing of quasicrystal in Ti-based Ti-Zr-Ni-Mg compound materials. International Conference on Mining, Material, and Metallurgical Engineering (ICMMME); April 22-23; Chiang Mai, Thailand, p. 42-45.
- Nobuki, T., Crivello, J.-C., Cuevas, F., and Joubert, J.-M. (2019). Fast synthesis of TiNi by mechanical alloying and its hydrogenation properties. *International J. Hydro. Energy.*, 44(21):10,770-10,776.
- Reilly, J.J. and Wiswall, R.H. (1968). The Reaction of Hydrogen with Alloys of Magnesium and Nickel and the Formation of Mg<sub>2</sub>NiH<sub>4</sub>. *Inorganic Chemistry.*, 07:2,254-2,256.
- Rongeat, C. and Roué, L. (2004). Effect of particle size on the electrode performance of MgNi hydrogen storage alloy. *J. Power Sources.*, 132(1-2):302-308.
- Samavat, F., Mohammad, H.T., Habibi, S., Jaleh, B., and Parisa, T.A. (2012). Quasicrystals. *J. Phys. Chem.*, 02:7-14.
- Shechtman, D., Blech, I., Gratias, D., and Cahn, J.W. (1984). Metallic phase with long-range orientational order and no translational symmetry. *Phys. Review Letters*, 53:1,951-1,953.
- Takasaki, A. and Kelton, K. (2006). Hydrogen storage in Ti-based quasicrystal powders produced by mechanical alloying. *Int. J. Hydro. Energy.*, 31:183-190.
- Takasaki, A., Huett, V.T., and Kelton, K.F. (2002). Hydrogenation of Ti-Zr-Ni quasicrystals synthesized by mechanical alloying. *J. Non-Crystalline Solids.*, 334-335: 457-60.
- Tominaga, T., Takasaki, A., Shibato, T., and Świerczek, K. (2015). HREM observation and high-pressure composition isotherm measurement of Ti<sub>45</sub>Zr<sub>38</sub>Ni<sub>17</sub> quasicrystal powders synthesized by mechanical alloying. *J. Alloy Comp.*, 645:S292-S294.
- Viano, A., Majzoub, E., Stroud, R., Kramer, M., Misture, S., Gibbons, P., and Kelton, K. (2010). Hydrogen absorption and storage in quasicrystalline and related Ti-Zr-Ni alloys. *Philosophical Magazine A*. 78(1):131-142.
- Wang, Y. and Wang Y. (2017). Recent advances in additive-enhanced magnesium hydride for hydrogen storage. *J. Mat. Int.*, 27:41-49.
- Xiangyu, Z., Liqun, M., Yao, Y., Ding, Y., and Xiaodong, S. (2010). Ti<sub>2</sub>Ni alloy: a potential candidate for hydrogen storage in nickel/metal hydride secondary batteries. *J. Energy Environ. Sci.*, 3:1,316-1,321.
- Zaluski, L., Zaluska A., and Strom-Olsen J.O. (1995). Hydrogen absorption in nanocrystalline Mg<sub>2</sub>Ni formed by mechanical alloying. *J Alloys Comp.*, 217:245-249.
- Zaluska, A., Zaluski, L., and Ström-Olsen, J. (1999). Synergy of hydrogen sorption in ball-milled hydrides of Mg and Mg<sub>2</sub>Ni. *J. Alloy Comp.*, 289(1-2):197-206.